

https://dspace.org/

Metaheuristic generation of brane tilings

Yang-Hui He; Vishnumohan Jejjala; Tomás S.R. Silva

ELSEVIER SCIENCE BV
https://hdl.handle.net/10539/46004
WOS

Downloaded from a DSpace repository. https://dspace.org/

Phys. Lett. B 862 (2025) 139365

Contents lists available at ScienceDirect

Physics Letters B

journal homepage: www.elsevier.com/locate/physletb

Letter

Metaheuristic generation of brane tilings

Yang-Hui He [a,b], Vishnu Jejjala [c], Tomás S.R. Silva [d,*]

[a] London Institute for Mathematical Sciences, Royal Institution, London, W1S 4BS, UK
[b] Merton College, University of Oxford, OX1 4JD, UK
[c] Mandelstam Institute for Theoretical Physics, School of Physics, NITheCS, and CoE-MaSS, University of the Witwatersrand, Johannesburg, WITS 2050, South Africa
[d] Instituto de Matemática, Estatística e Computação Científica (IMECC) da Universidade Estadual de Campinas (UNICAMP), 13083-859, Brazil

ARTICLE INFO

Editor: F. Bo

Dataset link: https://github.com/TomasSilva/Metaheuristic-brane-tiling-search

Dedicated to Professor Amihay Hanany, on the occasion of his 60th birthday
מזל טוב

Keywords:
Brane tilings
Permutation tuples
Simulated annealing

ABSTRACT

The combinatorics of dimer models on brane tilings describe a large class of four-dimensional $\mathcal{N} = 1$ gauge theories that afford quiver descriptions and have toric moduli spaces. We introduce a combinatorial optimization method leveraging simulated annealing to explicitly construct geometrically consistent brane tilings, providing a proof of concept for efficient generation of gauge theories using metaheuristic techniques. The implementation of this idea recovers known examples and allows us to derive a new brane tiling with 26 quantum fields, illustrating the potential of metaheuristic techniques as a valuable addition to the toolbox for constructing and analyzing gauge theories from brane tilings.

1. Introduction & summary

Brane tilings [1] reside at the intersection of the physics of supersymmetric quantum field theories [2,3], especially those obtained from string theory, the algebraic geometry of Calabi–Yau manifolds, particularly mirror symmetry and toric geometry [4–6], and the representation theory of quivers [7,8].

In its most canonical form, the brane tiling is a geometric and insightful way to encode the data of a $(3+1)$-dimensional supersymmetric gauge theory whose mesonic moduli space is a non-compact toric Calabi–Yau threefold. (See rapid review in [9] and the longer reviews [10,11].) The gauge theory data is a pair (Q, W) where Q is a direct graph (quiver) whose arrows are the fields and whose nodes are the gauge groups; and W is a superpotential which is a polynomial in the fields. The geometry data is a planar toric diagram — a convex lattice polygon — whose associated toric variety is a Fano surface over which the Calabi–Yau threefold is an affine cone. Realizing these $\mathcal{N} = 1$ theories as the worldvolume gauge theory on a D3-brane at the tip of a cone over a Sasaki–Einstein base, X, we have an infinite class of theories whose gravitational duals are known; they are $\mathrm{AdS}_5 \times X$ [12,13]. The graph dual to (Q, W) is a balanced bipartite graph drawn on T^2, known as a brane tiling or dimer model [3]. Given the combinatorial nature of the problem, it is natural that there have been catalogues of brane tilings [14–17].

The insight of [18–22] was that the data (Q, W) can be succinctly repackaged into a permutation triple, which weaves Grothendieck's *dessin d'enfants* and Belyi maps into the already rich tapestry. Here, the physics data is entirely captured by two lists of numbers, bypassing the complexities of graph adjacency or polynomials in arrows of graphs, in the following way. Fix the permutation group $\mathfrak{S}_d$ on d elements. Let σ_B and σ_W be two elements thereof, written explicitly in cycle-notation, and define $\sigma_F = (\sigma_B \sigma_W)^{-1}$. Then, the gauge theory has d fields with gauge group $\mathrm{SU}(N)^n$ where n is the number of cycles in σ_F and the superpotential terms are read off from the cycles in σ_B and σ_W.

The advent of AI driven discovery in theoretical physics and mathematics [23–27] (see reviews in [28–31]) has naturally led to the consideration of machine learning (ML) applied to the field of quivers, tilings and mutations, in the present context of string theory and in algebraic geometry [32–43]. It is therefore expedient to combine our two strands of thought: the efficient permutation triple representation of physics/mathematics, and the possibility of modeling the discovery of new quiver gauge theories as an optimization problem. This is the chief

* Corresponding author.
E-mail address: tomas@ime.unicamp.br (T.S.R. Silva).

https://doi.org/10.1016/j.physletb.2025.139365
Received 6 January 2025; Received in revised form 23 February 2025; Accepted 26 February 2025

Available online 27 February 2025
0370-2693/© 2025 The Author(s). Published by Elsevier B.V. Funded by SCOAP³. This is an open access article under the CC BY license (http://creativecommons.org/licenses/by/4.0/).

motivation of our work. In the remainder of this letter, we describe the encoding of a consistent brane tiling and employ simulated annealing techniques to generate new tilings.

2. Consistent tilings

As discussed in the introduction, brane tilings are efficiently encoded in terms of permutation tuples [18], whose consistency conditions are presented in [22]. In this section we summarize these conditions, with a view towards setting up the data.

Let d be the number of quantum fields. We take two elements of the symmetric group $\mathfrak{S}_d$, which we call σ_B and σ_W. The bipartite graph defining the theory has nodes that are colored black and white. Numbering the edges and reading these anticlockwise at the black nodes and clockwise at the white nodes recovers the two sets of gauge invariant operators that appear in the superpotential. That is to say, each cycle in σ_B and σ_W defines one term in the superpotential, and these are assigned couplings $+1$ and -1. As each edge connects a black node to a white node, each field appears twice in the superpotential, once with each sign. This is the essential requirement for a dimer model. The defining permutation tuples (σ_B, σ_W) satisfy the following consistency conditions.

PT-1 Two pairs of tuples (σ_B, σ_W) and (σ'_B, σ'_W) are equivalent when they are related by conjugation:

$$\sigma'_B = \gamma \sigma_B \gamma^{-1} , \quad \sigma'_W = \gamma \sigma_W \gamma^{-1} , \tag{1}$$

for some $\gamma \in \mathfrak{S}_d$. This ensures that the theory remains the same under a trivial relabeling of the fields.

PT-2 The group $G(\sigma_B, \sigma_W)$ whose generators are σ_B and σ_W is *transitive*. This means that for any pair of integers $i, j \in \{1, \ldots, d\}$ there exists $g \in G(\sigma_B, \sigma_W)$ such that g sends i to j.

PT-3 Define

$$\sigma_F := (\sigma_B \sigma_W)^{-1} . \tag{2}$$

Let C_σ count the number of cycles in σ. Then, from the Riemann–Hurwitz relations:

$$d - C_{\sigma_B} - C_{\sigma_W} - C_{\sigma_F} = 0 , \tag{3}$$

$$C_{\sigma_B} = C_{\sigma_W} . \tag{4}$$

Notice that (4) does not imply that the cycle structures of σ_B and σ_W are the same.

PT-4 The lengths of the cycles in σ_B and σ_W tell us how many fields appear in each term of the superpotential with $\pm$ signs, respectively. Twice the lengths of the cycles in σ_F tell us how many fields bound the faces of the associated bipartite graph.

PT-5 There are no one-cycles or two-cycles in either σ_B or σ_W as these would be tadpoles or mass terms.

We can algorithmically construct the zig-zag paths as an element of $\mathfrak{S}_{2d}$ [18]. Take the set

$$\Sigma = \{1^+, \ldots, d^+, 1^-, \ldots, d^-\} . \tag{5}$$

Define a permutation $\mathcal{Z}(\sigma_B, \sigma_W)$ of Σ by taking

$$\mathcal{Z}(k^-) = \sigma_B(k)^+ , \qquad \mathcal{Z}(k^+) = \sigma_W^{-1}(k)^- . \tag{6}$$

The cycles in $\mathcal{Z}(\sigma_B, \sigma_W^{-1})$ are the *zig-zag paths*. The cycles in $\mathcal{Z}(\sigma_B, \sigma_W)$ tell us which fields bound a face in the corresponding bipartite graph. (As the fields are bifundamental or adjoint, they correspond to edges that separate faces associated to the gauge groups; fixing an orientation, the two faces give a fundamental and an antifundamental index for the field.)

Let H be the Abelian group generated by $\sigma_B \sigma_W^{-1}$. We require the following two conditions.

CONS-1 For any $h \in H$, $h\sigma_B$ has no one-cycle. It is called a *derangement*.

CONS-2 Choose all pairs $(h_1, h_2) \in H \times H$. If $h_1 \sigma_B h_2 \sigma_W$ has one-cycles, these belong pairwise to zig-zag paths that are linearly dependent. *N.B.*: As this is only relevant for generating Seiberg dual phases, it is sufficient to demand that $h_1 \sigma_B h_2 \sigma_W$ be a derangement and then later apply *urban renewal* on the resulting bipartite graph [2,20].

For a physical theory, we compute R-charges associated to each of the fields by a-maximization [44]. These R-charges must satisfy the following conditions.

SUPER All the terms in the superpotential have R-charge 2. Thus, for each cycle in σ_B and σ_W:

$$2 = \sum_{a \in \text{cycle}} R(X_a) . \tag{7}$$

NSVZ The brane tiling admits an isoradial embedding on a flat torus. As noted above, the fields in $\mathcal{Z}(\sigma_B, \sigma_W)$ define the faces of the brane tiling. We require for each face

$$2 = \sum_{a \in \partial F_i} (1 - R(X_a)) . \tag{8}$$

This corresponds to the vanishing of the NSVZ beta functions.

3. Metaheuristic search for consistent permutation tuples

We now turn to ML and metaheuristic techniques to see whether we can efficiently generate permutation triples, and hence physical brane tilings, that satisfy all the conditions laid out in the previous section. After extensive experimentation with the likes of genetic algorithms and reinforcement learning environments, we found that the most efficient methods are metaheuristic ones as described in the ensuing.

Metaheuristics are high level probabilistic procedures, often inspired by natural phenomena, designed to find optimal solutions over large search spaces and have proven to be a successful alternative to classical approaches in combinatorial optimization (see [45] for a review). In particular, *Simulated Annealing* (SA) is a metaheuristic framework introduced in [46] that relies on a statistical model developed by [47]. SA emulates the thermodynamic process of *annealing*, representing the dynamics of particles within a heated solid as it progresses toward thermodynamic equilibrium.

In general, SA is guided by the principle of local search over a space (system) $\mathcal{S}$, using as control parameters a function $\texttt{Energy} : \mathcal{S} \to \mathbb{R}$ associated to any given state in $\mathcal{S}$ and a *temperature* $T^{(i)}$ related to the system in its i -th iteration. The objective is to find a state whose energy approximates the global minimum over the system. To do so, given an initial state in $\mathcal{S}$, at each iteration, a neighbor candidate solution y is computed based on the current solution x according to a function $\texttt{Move} : \mathcal{S} \to \mathcal{S}$. The current solution is updated if y has a lower energy than x. However, suppose y has a higher energy than x. In that case, the current solution is updated according to a probability distribution that depends on the i-th temperature of the system and the energy difference between x and y. This probabilistic swap avoids the algorithm being trapped in a local minimum. A pseudocode for a general implementation of SA is presented in Algorithm 1 of Appendix A.

Consider the problem of searching for geometrically consistent brane tilings encoded as permutation tuples, *i.e.*, finding pairs $(\sigma_B, \sigma_W) \in \mathfrak{S}_d \times \mathfrak{S}_d$ that satisfy the conditions outlined in §2. Among these, **PT-1** imposes a double-conjugation condition, a standard criterion in permutation group theory to establish equivalence among known consistent tuples. Similarly, **PT-4** relates the cycle lengths within the tuple to the structure of the induced quiver. However, these conditions do not contribute to the construction of new consistent tuples.

Therefore, to identify geometrically consistent tilings, we proceed as follows. The permutations σ_B and σ_W are represented as lists of subsets of integers from 1 to d, corresponding to their cycle decompositions. The

primary goal is to satisfy the conditions **PT-2**, **PT-3**, **PT-5**, **CONS-1**, and **CONS-2**. Notably, since any brane tiling that can be mapped onto a torus inherently exhibits locally flat nodes and faces, the **SUPER** and **NSVZ** conditions are automatically satisfied [22]. Our method then searches for permutations that yield a physically valid brane tiling, with **PT-1** applied at the end to eliminate redundancies.

It is worth noting that a naïve brute force approach to this problem becomes computationally infeasible as the number of quantum fields d increases, with an expected complexity of $O((d!)^2)$. To address this, we propose a combinatorial optimization method based on simulated annealing (SA) to efficiently search for consistent tilings with large d using finite computational resources.

Therefore, we need to define a suitable energy function that captures how close a given permutation tuple (σ_B, σ_W) in the search space $\mathcal{S} = \mathfrak{S}_d \times \mathfrak{S}_d$ is from being consistent, so that finding a global minimum for this function corresponds to finding a consistent tiling. This is achieved using routines `PT-2 Score`, `PT-3 Score`, `PT-5 Score`, `CONS-1 Score`, and `CONS-2 Score` (detailed in Appendix A), which implement, respectively, scoring routines that measure some *proximity* notion of fulfilling each of **PT-2**, **PT-3**, **PT-5**, **CONS-1**, and **CONS-2**; so that a score equals to one is assigned if the correspondent condition is satisfied, and $0 < \texttt{score} < 1$ otherwise.

With these score functions in hand, we can define a function $\texttt{Energy} : \mathfrak{S}_d \times \mathfrak{S}_d \to [0, 6)$ as:

$$\begin{aligned}\texttt{Energy}(\sigma_B, \sigma_W) = 6 &- (\texttt{PT-2 Score})(\sigma_B, \sigma_W) \\ &- (\texttt{PT-3a Score})(\sigma_B, \sigma_W) \\ &- (\texttt{PT-3b Score})(\sigma_B, \sigma_W) \\ &- (\texttt{PT-5 Score})(\sigma_B, \sigma_W) \\ &- (\texttt{CONS-1 Score})(\sigma_B, \sigma_W) \\ &- (\texttt{CONS-2 Score})(\sigma_B, \sigma_W).\end{aligned} \tag{9}$$

For some d, the energy function defined in (9) takes a permutation tuple $(\sigma_B, \sigma_W) \in \mathfrak{S}_d \times \mathfrak{S}_d$ and assigns a value in the range $[0, 6)$. The energy associated with a state is zero if, and only if, all consistency conditions are simultaneously satisfied, and it is higher as the number of conditions not (partially) satisfied by a state tuple increases.

It is important to note that during our experiments the partial scoring approach as in (9) outperformed binary counting of the total consistency conditions satisfied by a given state. The key difference lies in the smoothness of the energy evaluation between the current solution and a random neighbor. A smoother transition in energy values is crucial for obtaining more reliable estimates of the global minimum of the energy function, corresponding to finding states with zero energy (i.e., consistent tilings).

The remaining component we need to define for executing our SA routine is an appropriate `Move` function, that produces random neighbors of a given state. There are many possible ways to define such a function in our search space $\mathcal{S} = \mathfrak{S}_d \times \mathfrak{S}_d$ of pairs of permutations, e.g. by randomly shuffling each component of the tuple (σ_B, σ_W); or by swapping two random elements in each component σ_B and σ_W. However, these do not guarantee the preservation of the cycle structure in the state to be moved and often generate pairs that trivially do not satisfy some cycle-type consistency conditions. Given the $O((d!)^2)$ nature of our search space, we want to avoid as many trivial unnecessary checks as possible. Thus, we designed a `Move` algorithm that preserves the cycle structure of a given initial state and therefore does not mishandle previously user-imposed conditions as **PT-3** (4) and **PT-5**. This is exhibited in Algorithm 8 of Appendix A.

Finally, we mention that both the number of iteration N and the cooling schedule in our SA approach (as in Algorithm 1, Appendix A) need to be fine tuned, with optimal performance varying according to the number of quantum fields d that we want to work on. The initial-state (σ_B, σ_W) cycle structure must also be adjusted. A SageMath [48] implementation of the routines discussed here is available on the following GitHub repository: https://github.com/TomasSilva/Metaheuristic-brane-tiling-search.

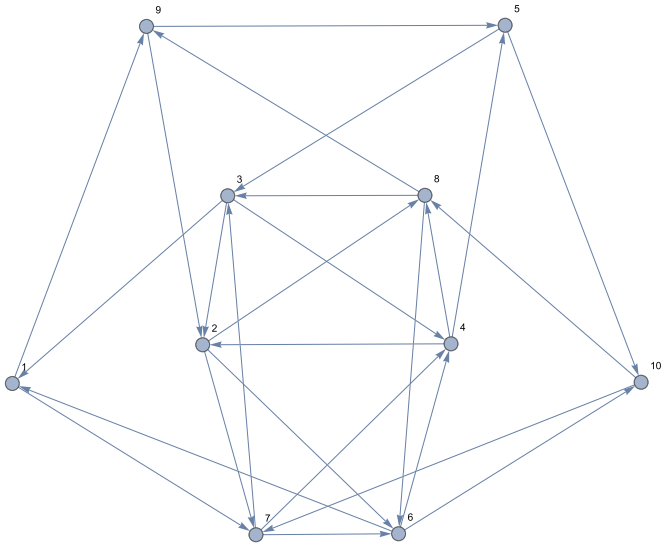


Fig. 1. Quiver induced from the permutation tuple in (10).

4. Results

With our SA approach, we were able to reproduce most of the consistent brane tiling presented in previous catalogues [14,16] up to **PT-1** equivalence.

In order to generate new examples of tilings, we focused on optimizing our algorithm for larger numbers of quantum fields, for which no complete classification catalogue is known. We emphasize that our metaheuristic SA search for consistent brane tilings with a large number of fields d is still a computationally intensive task since the number of iterations N required by our algorithm to converge to zero-energy states scales significantly with d.

Below, we present a new example of consistent brane tiling with $d = 26$ quantum fields obtained through our SA approach. This example is not listed (up to equivalence **PT-1**) in previous catalogues as [14,16,17], which were classifications up to 24 fields. Thus, this supplies a proof of principle for generating explicit $\mathcal{N} = 1$ gauge theories (dimer models) from metaheuristics.

$$\begin{aligned}\sigma_B =&(1,3,21,14)(2,4,8)(5,19,24,26)(6,7,25)\\ &(9,17,11)(10,23,18)(12,22,16)(13,15,20)\\ \sigma_W =&(1,10,2,6)(3,25,16)(4,12,24)(5,20,23,14)\\ &(7,13,26)(8,17,15)(9,22,18)(11,19,21)\end{aligned} \tag{10}$$

We can readily write the superpotential from the permutation triples in (10). First, there are ten gauge group factors, as shown in the quiver diagram in Fig. 1. In standard notation $X_{i,j}$ is a bifundamental field from the i-th gauge group $SU(N_i)$ to the j-th (and noting that there are no adjoint fields $\phi_{i,i}$ corresponding to self-joining loops at a node in the quiver), we can write the 16-term superpontential, consisting of six pairs of cubic interactions and two pairs of quartic, as

$$\begin{aligned}W =& X_{3,1}X_{7,3}X_{1,7} - X_{2,6}X_{4,2}X_{6,4} - X_{2,7}X_{3,2}X_{7,3} + X_{3,4}X_{5,3}X_{4,5}\\ &- X_{6,10}X_{8,6}X_{10,8} - X_{6,1}X_{7,6}X_{1,7} + X_{4,2}X_{7,4}X_{2,7} + X_{6,4}X_{8,6}X_{4,8}\\ &+ X_{7,6}X_{10,7}X_{6,10} + X_{8,3}X_{2,8}X_{3,2} - X_{9,2}X_{8,9}X_{2,8} - X_{8,3}X_{4,8}X_{3,4}\\ &+ X_{1,9}X_{6,1}X_{2,6}X_{9,2} - X_{1,9}X_{3,1}X_{5,3}X_{9,5}\\ &+ X_{5,10}X_{9,5}X_{8,9}X_{10,8} - X_{5,10}X_{4,5}X_{7,4}X_{10,7}\,.\end{aligned} \tag{11}$$

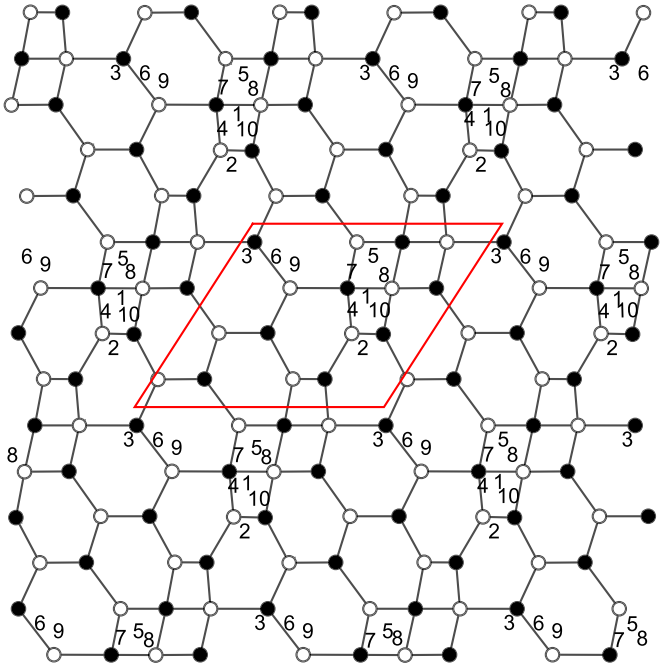


Fig. 2. Tiling induced from the permutation tuple in (10).

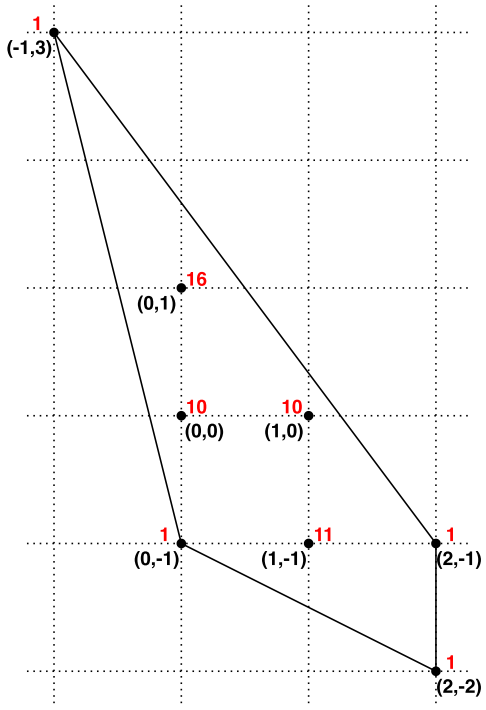


Fig. 3. Toric diagram induced from the permutation tuple in (10), with multiplicities in red.

The brane tiling, which is the dual graph to the (periodic version of the) quiver together with the superpotential, is drawn as a dimer model on the torus in Fig. 2, where the red parallelogram marks the fundamental domain. The moduli space, which can be computed using the forward algorithm, is an affine toric Calabi–Yau threefold, whose planar toric diagram is given in Fig. 3. We have marked the multiplicity of GLSM fields associated to each point on the toric diagram — these should count the perfect matchings in the dimer model. In all, the points of the toric diagram and the corresponding number of perfect matchings are:

Lattice Point	GLSM/Perfect Matching
$(0,1)$	16
$(1,-1)$	11
$(0,0),\ (1,0)$	10
$(2,-2),\ (0,-1),\ (-1,3),\ (2,-1)$	1

(12)

We note that the four external vertices in the toric diagram, *viz.*, $\{(2,-2),\ (0,-1),\ (-1,3),\ (2,-1)\}$ all have multiplicity 1. This is consistent with all known theories. We also note that there are four internal points, and the origin $(0,0)$ is taken to be one of the interior points by convenient choice. Although there are many known brane tilings for toric diagrams with large numbers of internal points (*e.g.*, $Y^{p,q}$ [2] and $L^{a,b,c}$ [49]), this theory did not appear in any of the previous catalogues [14–17] that are primarily concerned with reflexive (single interior point) and two interior points, or with going up in the area of the toric diagram.

We can read off the geometry from the toric diagram and using the toric varieties modules of SageMath [48]. Taking the face fan of the lattice polytope, we see that the fan is composed of 4 affine cones, defined cyclically by taking neighboring rays in $\{(0,-1),\ (1,-1),\ (2,-1),\ (-1,3)\}$. This defines a non-smooth complex surface B overwhich the (Higgs Branch) moduli space is an affine cone which is a non-compact Calabi–Yau threefold X. The (singular) Euler number of B is computed to be $16/5$.

We can construct the cone X as an affine toric variety by adding a coordinate and keep the endpoints co-planar in order to preserve the Calabi–Yau condition. For instance, we can just append 1 to the two-dimensional lattice points. This allows one of write down X as a (non-complete) intersection of 72 polynomials in $\mathbb{C}^{12}$. One can compute the refined Hilbert series for X using [50,51] directly from reading the toric diagram. This depends on the triangulation; taking the incidence of the triangulation on the 8 lattice points as $<0,1,3>, <0,3,7>, <1,3,7>, <1,6,7>$, we have

$$\begin{aligned} HS(X;t_{1,2,3}) = &\frac{t_1^2 t_2^2 t_3^4}{\left(1-t_1^2\right)\left(t_1^2 t_2^2 - t_3^2\right)\left(t_2^2 t_3^2 - 1\right)} \\ &+ \frac{t_1^4 t_2 t_3^2}{\left(t_1^2 - 1\right)\left(t_1^2 t_2 - t_3\right)\left(t_1^4 t_2 t_3 - 1\right)} \\ &- \frac{t_1^4 t_2^3 t_3^5}{\left(t_1^2 t_2 - t_3\right)\left(t_1^2 t_2^2 - t_3^2\right)\left(t_1^4 t_2^3 - t_3^5\right)} \\ &+ \frac{t_1 t_2^2 t_3^4}{\left(t_1 - t_3^2\right)\left(t_2^2 t_3^2 - 1\right)\left(t_1 t_2^2 t_3^2 - 1\right)} \end{aligned} \tag{13}$$

Declaration of competing interest

The authors declare the following financial interests/personal relationships which may be considered as potential competing interests: Tomas S. R. Silva reports financial support was provided by State of São Paulo Research Foundation grant 2022/09891-4. Yang-Hui He reports financial support was provided by Leverhulme Trust grant "Topology from cosmology: axions, astrophysics and machine learning". If there are other authors, they declare that they have no known competing financial interests or personal relationships that could have appeared to influence the work reported in this paper.

Acknowledgements

We thank Jurgis Pasukonis and Xiao Yan for the code for visualizing the dimers. YHH is supported by the STFC UK for grant ST/J00037X/2 and a Leverhulme project grant "Topology from cosmology: axions, astrophysics and machine learning". VJ acknowledges the South African

Research Chairs Initiative of the Department of Science and Innovation and the National Research Foundation. TSRS is supported by the São Paulo Research Foundation (FAPESP) grant 2022/09891-4, and highlights that this research utilized computational resources of the "*Centro Nacional de Processamento de Alto Desempenho em São Paulo* (CENAPAD-SP)".

Appendix A. Supplementary material

Supplementary material related to this article can be found online at https://doi.org/10.1016/j.physletb.2025.139365.

Data availability

Code and Data available at: https://github.com/TomasSilva/Metaheuristic-brane-tiling-search (also quoted in paper).

References

[1] A. Hanany, K.D. Kennaway, Dimer models and toric diagrams, arXiv:hep-th/0503149, 3 2005.
[2] S. Franco, A. Hanany, K.D. Kennaway, D. Vegh, B. Wecht, Brane dimers and quiver gauge theories, J. High Energy Phys. 01 (2006) 096, arXiv:hep-th/0504110.
[3] S. Franco, A. Hanany, D. Martelli, J. Sparks, D. Vegh, B. Wecht, Gauge theories from toric geometry and brane tilings, J. High Energy Phys. 01 (2006) 128, arXiv:hep-th/0505211.
[4] B. Feng, A. Hanany, Y.-H. He, D-brane gauge theories from toric singularities and toric duality, Nucl. Phys. B 595 (2001) 165–200, arXiv:hep-th/0003085.
[5] B. Feng, Y.-H. He, K.D. Kennaway, C. Vafa, Dimer models from mirror symmetry and quivering amoebae, Adv. Theor. Math. Phys. 12 (3) (2008) 489–545, arXiv:hep-th/0511287.
[6] A. Hanany, R.-K. Seong, Brane tilings and specular duality, J. High Energy Phys. 08 (2012) 107, arXiv:1206.2386.
[7] C. Beil, Cyclic contractions of dimer algebras always exist, Algebr. Represent. Theory 22 (5) (2019) 1083–1100, arXiv:1703.04450.
[8] S. Franco, G. Musiker, Higher cluster categories and QFT dualities, Phys. Rev. D 98 (4) (2018) 046021, arXiv:1711.01270.
[9] Y.-H. He, Calabi-Yau varieties: from quiver representations to dessins d'Enfants, arXiv:1611.09398, 11 2016.
[10] K.D. Kennaway, Brane tilings, Int. J. Mod. Phys. A 22 (2007) 2977–3038, arXiv:0706.1660.
[11] M. Yamazaki, Brane tilings and their applications, Fortschr. Phys. 56 (2008) 555–686, arXiv:0803.4474.
[12] I.R. Klebanov, E. Witten, Superconformal field theory on three-branes at a Calabi-Yau singularity, Nucl. Phys. B 536 (1998) 199–218, arXiv:hep-th/9807080.
[13] S. Benvenuti, S. Franco, A. Hanany, D. Martelli, J. Sparks, An infinite family of superconformal quiver gauge theories with Sasaki-Einstein duals, J. High Energy Phys. 06 (2005) 064, arXiv:hep-th/0411264.
[14] J. Davey, A. Hanany, J. Pasukonis, On the classification of brane tilings, J. High Energy Phys. 01 (2010) 078, arXiv:0909.2868.
[15] A. Hanany, R.-K. Seong, Brane tilings and reflexive polygons, Fortschr. Phys. 60 (2012) 695–803, arXiv:1201.2614.
[16] S. Franco, Y.-H. He, C. Sun, Y. Xiao, A comprehensive survey of brane tilings, Int. J. Mod. Phys. A 32 (23n24) (2017) 1750142, arXiv:1702.03958.
[17] J. Bao, G.B. Colverd, Y.-H. He, Quiver gauge theories: beyond reflexivity, J. High Energy Phys. 2020 (6) (Jun. 2020).
[18] V. Jejjala, S. Ramgoolam, D. Rodriguez-Gomez, Toric CFTs, permutation triples and belyi pairs, J. High Energy Phys. 03 (2011) 065, arXiv:1012.2351.
[19] A. Hanany, Y.-H. He, V. Jejjala, J. Pasukonis, S. Ramgoolam, D. Rodriguez-Gomez, The beta ansatz: a tale of two complex structures, J. High Energy Phys. 06 (2011) 056, arXiv:1104.5490.
[20] A. Hanany, Y.-H. He, V. Jejjala, J. Pasukonis, S. Ramgoolam, D. Rodriguez-Gomez, Invariants of toric Seiberg duality, Int. J. Mod. Phys. A 27 (2012) 1250002, arXiv:1107.4101.
[21] Y.-H. He, V. Jejjala, D. Rodriguez-Gomez, Brane geometry and dimer models, J. High Energy Phys. 06 (2012) 143, arXiv:1204.1065.
[22] A. Hanany, V. Jejjala, S. Ramgoolam, R.-K. Seong, Consistency and derangements in brane tilings, J. Phys. A 49 (35) (2016) 355401, arXiv:1512.09013.
[23] Y.-H. He, Deep-learning the landscape, Phys. Lett. B 774 (2017) 564–568, arXiv:1706.02714.
[24] D. Krefl, R.-K. Seong, Machine learning of Calabi-Yau volumes, Phys. Rev. D 96 (6) (2017) 066014, arXiv:1706.03346.
[25] D. Aggarwal, Y.-H. He, E. Heyes, E. Hirst, H.N. Sá Earp, T.S.R. Silva, Machine learning Sasakian and G_2 topology on contact Calabi-Yau 7-manifolds, Phys. Lett. B 850 (2024) 138517.
[26] J. Carifio, J. Halverson, D. Krioukov, B.D. Nelson, Machine learning in the string landscape, J. High Energy Phys. 09 (2017) 157, arXiv:1707.00655.
[27] F. Ruehle, Evolving neural networks with genetic algorithms to study the string landscape, J. High Energy Phys. 08 (2017) 038, arXiv:1706.07024.
[28] Y.-H. He, The Calabi–Yau Landscape: From Geometry, to Physics, to Machine Learning, Lecture Notes in Mathematics, 2021, arXiv:1812.02893.
[29] F. Ruehle, Data science applications to string theory, Phys. Rep. 839 (2020) 1–117.
[30] S. Gukov, J. Halverson, F. Ruehle, Rigor with machine learning from field theory to the Poincaré conjecture, Nat. Rev. Phys. (2024) 1–10.
[31] Y.-H. He, AI-driven research in pure mathematics and theoretical physics, Nat. Rev. Phys. 6 (9) (2024) 546–553, arXiv:2405.19973.
[32] Y.-H. He, E. Hirst, T. Peterken, Machine-learning dessins d'enfants: explorations via modular and Seiberg–Witten curves, J. Phys. A 54 (7) (2021) 075401, arXiv:2004.05218.
[33] J. Bao, S. Franco, Y.-H. He, E. Hirst, G. Musiker, Y. Xiao, Quiver mutations, Seiberg duality and machine learning, Phys. Rev. D 102 (8) (2020) 086013, arXiv:2006.10783.
[34] J. Bao, Y.-H. He, E. Hirst, Neurons on amoebae, J. Symb. Comput. 116 (2023) 1–38, arXiv:2106.03695.
[35] G. Arias-Tamargo, Y.-H. He, E. Heyes, E. Hirst, D. Rodriguez-Gomez, Brain webs for brane webs, Phys. Lett. B 833 (2022) 137376, arXiv:2202.05845.
[36] S. Chen, Y.-H. He, E. Hirst, A. Nestor, A. Zahabi, Mahler measuring the genetic code of amoebae, Adv. Theor. Math. Phys. 27 (5) (2023) 1405–1461, arXiv:2212.06553.
[37] M.-W. Cheung, P.-P. Dechant, Y.-H. He, E. Heyes, E. Hirst, J.-R. Li, Clustering cluster algebras with clusters, Adv. Theor. Math. Phys. 27 (3) (2023) 797–828, arXiv:2212.09771.
[38] P.-P. Dechant, Y.-H. He, E. Heyes, E. Hirst, Cluster algebras: network science and machine learning, J. Comput. Algebra 8 (2023), arXiv:2203.13847.
[39] R.-K. Seong, Unsupervised machine learning techniques for exploring tropical coamoeba, brane tilings and Seiberg duality, Phys. Rev. D 108 (10) (2023) 106009, arXiv:2309.05702.
[40] J. He, H. Jenne, H. Chau, D. Brown, M. Raugas, S. Billey, H. Kvinge, Machines and mathematical mutations: using GNNs to characterize quiver mutation classes, arXiv:2411.07467, 11 2024.
[41] K.T.K. Armstrong-Williams, E. Hirst, B. Jackson, K.-H. Lee, Machine learning mutation-acyclicity of quivers, arXiv:2411.04209, 11 2024.
[42] R.-K. Seong, Generative AI for brane configurations, tropical coamoeba and 4d N = 1 quiver gauge theories, arXiv:2411.16033, 11 2024.
[43] S. Gukov, R.-K. Seong, Machine learning BPS spectra and the gap conjecture, Phys. Rev. D 110 (4) (2024) 046016, arXiv:2405.09993.
[44] K.A. Intriligator, B. Wecht, The exact superconformal R symmetry maximizes a, Nucl. Phys. B 667 (2003) 183–200, arXiv:hep-th/0304128.
[45] L. Bianchi, M. Dorigo, L.M. Gambardella, W.J. Gutjahr, A survey on metaheuristics for stochastic combinatorial optimization, Nat. Comput. 8 (2) (2008) 239–287.
[46] S. Kirkpatrick, C.D. Gelatt, M.P. Vecchi, Optimization by simulated annealing, Science 220 (4598) (1983) 671–680.
[47] N. Metropolis, A.W. Rosenbluth, M.N. Rosenbluth, A.H. Teller, E. Teller, Equation of state calculations by fast computing machines, J. Chem. Phys. 21 (6) (1953) 1087–1092.
[48] T.S. Developers, W. Stein, D. Joyner, D. Kohel, J. Cremona, B. Eröcal, SageMath, version 9.0 http://www.sagemath.org, 2020.
[49] M. Cvetič, H. Lü, D.N. Page, C.N. Pope, New Einstein-Sasaki spaces in five and higher dimensions, Phys. Rev. Lett. 95 (7) (Aug. 2005), https://doi.org/10.1103/PhysRevLett.95.071101.
[50] S. Benvenuti, B. Feng, A. Hanany, Y.-H. He, Counting BPS operators in gauge theories: quivers, syzygies and plethystics, J. High Energy Phys. 11 (2007) 050, arXiv:hep-th/0608050.
[51] Y.-H. He, R.-K. Seong, S.-T. Yau, Calabi–Yau volumes and reflexive polytopes, Commun. Math. Phys. 361 (1) (2018) 155–204, arXiv:1704.03462.